Diffusion tensor imaging segmentation by watershed transform on tensorial morphological gradient

Leticia Rittner and Roberto Lotufo
School of Electrical and Computer Engineering
University of Campinas - UNICAMP
C.P. 6101, 13083-852, Campinas (SP), Brazil
lrittner@dca.fee.unicamp.br, www.dca.fee.unicamp.br/∼lotufo

Abstract

While scalar image segmentation has been studied extensively, diffusion tensor imaging (DTI) segmentation is a relatively new and challenging task. Either existent segmentation methods have to be adapted to deal with tensorial information or completely new segmentation methods have to be developed to accomplish this task. Alternatively, what this work proposes is the computation of a tensorial morphological gradient of DTI, and its segmentation by IFT-based watershed transform. The strength of the proposed segmentation method is its simplicity and robustness, consequences of the tensorial morphological gradient computation. It enables the use, not only of well known algorithms and tools from the mathematical morphology, but also of any other segmentation method to segment DTI, since the computation of the tensorial morphological gradient transforms tensorial images in scalar ones. In order to validate the proposed method, synthetic diffusion tensor fields were generated, and Gaussian noise was added to them. A set of real DTI was also used in the method validation. All segmentation results confirmed that the proposed method is capable to segment different diffusion tensor images, including noisy and real ones.

1 Introduction

Diffusion tensor imaging (DTI) is a relatively new modality of Magnetic Resonance Imaging (MRI) able to quantify the anisotropic diffusion of water molecules in highly structured biological tissues. It is unique in its ability to quantify changes in neural tissue microstructure within the human brain non-invasively. Diffusion tensor imaging (DTI) segmentation, where regions of interest are delineated, is necessary for performing subsequent quantitative analysis and qualitative visualization. While scalar image segmentation has been studied extensively and different algorithms have been developed over a long period of time, DTI segmentation is a relatively new and challenging task and only a few different approaches for DTI segmentation have been proposed in the last decade [22, 23, 20, 19, 2, 21].

This work describes an approach to DTI segmentation using concepts from mathematical morphology [8] and from the Image Foresting Transform (IFT) [10]. And the image edge enhancement by gradient computation is an important step in morphological image segmentation via IFT-based watershed transform [14, 15]. For scalar images, the morphological gradient [12] is a very good option and its computation is simple: for each point in the image, a structuring element is centered to it and the difference between the maximum and the minimum graylevels inside the structuring element is computed. Here, the dissimilarity information exploited is the intensity difference among pixels inside the structuring element.

Such concept does not extend naturally to tensorial images. Although the dissimilarity information is richer in tensorial images than in scalar ones, the design of methods to edge enhancement in tensorial images is complex. Note that measures that compute the dissimilarity information of tensorial images are not natural for the human eye. Not to mention that information contained in the diffusion tensors is complex, and is still unknown which information is important for segmentation purposes and which can (and should) be ignored. Furthermore, either existing segmentation methods have to be adapted to deal with tensorial information or completely new segmentation methods have to be developed to accomplish this task.

Alternatively, what this work proposes is the computation of a gradient, that transforms the diffusion tensor image into an scalar image, and makes possible the use of any existing segmentation method in order to perform the DTI segmentation. With this in mind, the tensorial morphological gradient is employed. The tensorial morphological gra-

dient was first applied to tensorial images representing color images [17], but its concept can be extended and applied to any kind of tensorial image.

This paper is organized as follows: Section 2 describes the tensorial morphological gradient (TMG) after presenting a summary of basic concepts related to it. Section 3 presents the TMG applied to diffusion tensor images, through examples of synthetic and real tensorial images. Section 4 contains the segmentation results, obtained by the application of well-known segmentation techniques, such as IFT-based watershed transform and threshold, on the tensorial morphological gradient of diffusion tensor images. Finally, conclusions are summarized in Section 5.

2 Tensorial Morphological Gradient (TMG)

Although measures that computes the dissimilarity information of tensorial images are not natural for the human eye, by using them to compute a tensorial morphological gradient, it is possible to obtain an scalar image that can be interpreted as a border enhancement of the original tensorial image. Before explaining the tensorial morphological gradient (TMG), basic concepts regarding diffusion tensors, tensorial similarity measures and morphological gradient are briefly described.

2.1 Diffusion Tensors

A tensor is the mathematical idealization of a geometric or physical quantity whose analytic description, relative to a fixed frame of reference, consists of an array of numbers. In other words, it is an abstract object expressing some definite type of multi-linear concept. Its well-known properties can be derived from its definitions and the rules for manipulation of tensors arise as an extension of linear algebra to multilinear algebra [6].

Diffusion Tensor Imaging (DTI) is based on second order tensors. In practice, a 3-dimensional second order tensor is denoted by a 3×3 matrix of values:

$$\mathbf{T} = \begin{pmatrix} T_{xx} & T_{xy} & T_{xz} \\ T_{yx} & T_{yy} & T_{yz} \\ T_{zx} & T_{zy} & T_{zz} \end{pmatrix}, \tag{1}$$

and can be reduced to principal axes (eigenvalue and eigenvector decomposition) by solving the characteristic equation:

$$\mathbf{T} - (\lambda \cdot \mathbf{I})e = 0, \tag{2}$$

where $\mathbf{I}$ is the identity matrix, λ are the eigenvalues of the tensor and e are the normalized eigenvectors. Because de diffusion tensor is a symmetric positive definite matrix,i.e., $T_{xy} = T_{yx}$, $T_{yz} = T_{zy}$ and $T_{xz} = T_{zx}$ the eigenvalues are always real. Moreover, the corresponding eigenvectors are orthogonal [4]. In this case, the tensor can be represented by an ellipsoid, where the main hemiaxis lengths are proportional to the square roots of the tensor eigenvalues λ_1, λ_2 and λ_3 ($\lambda_1 \geq \lambda_2 \geq \lambda_3$) and their direction correspond to the respective eigenvectors (Fig. 1).

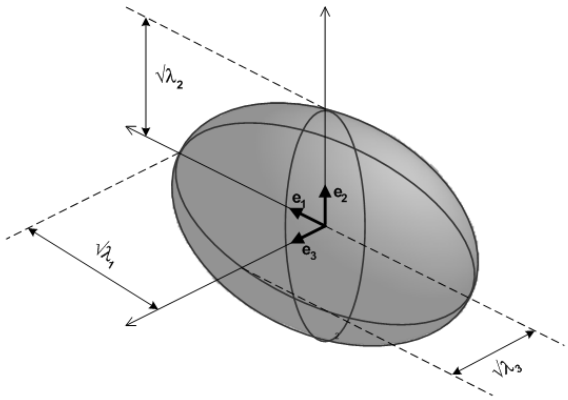

Figure 1. Ellipsoid representing a tensor

The degree of anisotropy in the diffusion ellipsoid, as represented by the tensor, can be quantified in a single number called a diffusion anisotropy index. The most widely used diffusion anisotropy index is probably the fractional anisotropy (FA), described by Basser and Pierpaoli in [3]. It ranges from 0 (isotropic diffusion) to 1 (completely anisotropic diffusion) and is defined by:

$$FA = \sqrt{\frac{3[(\lambda_1 - \mathbf{T}_{av})^2 + (\lambda_2 - \mathbf{T}_{av})^2 + (\lambda_3 - \mathbf{T}_{av})^2]}{2(\lambda_1^2 + \lambda_2^2 + \lambda_3^2)}}, \tag{3}$$

where

$$\mathbf{T}_{av} = \frac{\lambda_1 + \lambda_2 + \lambda_3}{3}. \tag{4}$$

The fractional anisotropy of a diffusion tensor, as proposed in [3], characterize geometrically the shape of the ellipsoid, but not its size or orientation.

The sum of the diagonal elements, also called trace, is another property of the diffusion tensor, and can be useful in comparing different tensors and ellipsoids. For a given 3×3 tensor, the trace of the ellipsoid can be calculated as follows:

$$Trace = (\lambda_1 + \lambda_2 + \lambda_3), \tag{5}$$

The trace of a diffusion tensor can be geometrically interpreted as the size of the ellipsoid, independent of shape and orientation.

2.2 Tensorial similarity measures

Since a key factor in DTI analysis is the proper choice of the similarity measure to be used, several works have been published on the subject. Given two tensors $\mathbf{T}_i$ e $\mathbf{T}_j$, the most simple comparison between two tensor quantities is the dot product between the principal eigenvector directions:

$$d_1(\mathbf{T}_i, \mathbf{T}_j) = |e_{1,i} \cdot e_{1,j}|, \tag{6}$$

where $e_{1,i}$ and $e_{1,j}$ are the principal eigenvectors of tensors $\mathbf{T}_i$ e $\mathbf{T}_j$, respectively. The absolute value of the dot product solves the problem with the sign ambiguity of the eigenvectors. This measure was used by Ziyan *et al.* to segment the thalamic nuclei from diffusion tensor images [23].

Another simple similarity measure, presented by Pierpaoli *et al.* as an intervoxel anisotropy index [16] and used by Alexander *et al.* [1], is the tensor dot product:

$$d_2(\mathbf{T}_i, \mathbf{T}_j) = \lambda_{1,i}\lambda_{1,j}(e_{1,i} \cdot e_{1,j})^2 + \lambda_{2,i}\lambda_{2,j}(e_{2,i} \cdot e_{2,j})^2. \tag{7}$$

In [1] Alexander *et al.* proposed another similarity measures. Their purpose was to match pairs of diffusion tensor images (DTI) and the proposed measures were based on the diffusion tensor itself and indices derived from the diffusion tensor. One of the similarity measures proposed by them was obtained negating the following Euclidean distance metric:

$$d_3(\mathbf{T}_i, \mathbf{T}_j) = \sqrt{\text{Trace}((\mathbf{T}_i - \mathbf{T}_j)^2)}, \tag{8}$$

This similarity metric was also explored in other DTI studies under different names, such as generalized tensor dot product [7] and Frobenius norm [21, 23]. But because affine invariance is a desirable property for segmentation purposes and the Frobenius norm is not invariant to affine transformations, Wang and Vemuri [19] proposed a novel definition of diffusion tensor "distance", as the square root of the J-divergence of the corresponding Gaussian distributions, i.e.,

$$d_4(\mathbf{T}_i, \mathbf{T}_j) = \frac{1}{2}\sqrt{\text{Trace}(\mathbf{T}_i^{-1}\mathbf{T}_j - \mathbf{T}_j^{-1}\mathbf{T}_i) - 2n}. \tag{9}$$

Eq. 9 is not a true distance since it violates the triangle inequality, but it is in fact a computationally efficient approximation of Rao's distance [19].

The above similarity measures are not the only ones proposed in the literature, but they were chosen to be part of this study because of their simplicity and/or their good performance, when dealing with diffusion tensor imaging applications. It is important to notice that each one of them come from different approaches and privileges some aspects of tensors. For example, whereas the dot product takes in account only the principal eigenvector direction, the tensor dot product and the Frobenius norm use the full tensor information.

2.3 Morphological gradient

Several distinct gradients are used in image processing to detect edges. One of them is called the morphological gradient, that depends on the size and shape of the chosen structuring element. Using a flat structuring element at each point, the morphological gradient yields the difference between the maximum and the minimum values over the neighborhood at the point determined by the flat structuring element [12]. The use of a three-dimensional structuring element leads to a morphological gradient that takes into account the neighborhood in all directions, and not only in an specific plane.

2.4 Tensorial morphological gradient (TMG)

The tensorial morphological gradient (TMG) was first described in [17] and used, together with a tensorial representation of colors, to segment color images. Let $E = \mathbb{Z}\times\mathbb{Z}$ be the set of all points in the tensorial image f. The tensorial morphological gradient (TMG) is defined by

$$\nabla_B^T(f)(x) = \bigvee_{y,z\in B_x} d_n(\mathbf{T}_y, \mathbf{T}_z) \tag{10}$$

$\forall x \in E$, where d_n represent any of the similarity measures presented in Subsection 2.2, $B \subset E$ is a structured element centered at the origin of E, $\mathbf{T}_y$ is the tensor that represents the diffusion in y, and $\mathbf{T}_z$ is the tensor that represents the diffusion in z (y and z are in the neighborhood of x, defined by E). ∇_B^T is the proposed TMG.

Because the chosen measures are already comparisons between neighbors, the proposed gradient is not the difference between the maximum and the minimum values, as in the classical morphological gradient, but only the maximum value. In other words, the computed gradient in a neighborhood given by an structuring element is the maximum dissimilarity among all pairwise dissimilarities.

So the main requirement of the TMG is that it must retain as much information from the tensors as possible. In other words, in order to compute the TMG the chosen similarity measure must take into account the most important characteristics of diffusion tensors, when compared to one another.

3 Tensorial morphological gradient of diffusion tensor images

As stated before, the tensorial morphological gradient (TMG) was first applied to tensorial images representing color images [17], but its concept can be extended and applied to any kind of tensorial image.

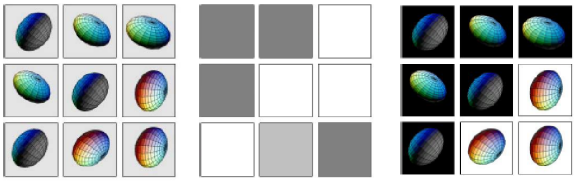

(a) Tensorial image (b) TMG (c) Segmented image

Figure 2. Representation of a tensorial image segmentation based on TMG

Fig. 2 depicts the idea behind the proposed tensorial morphological gradient (TMG) [1]. Fig. 2(a) shows an example of a 3×3 tensorial image, where instead of scalar values, each pixel of the image contains a tensor, i.e., a symmetric positive definite 3×3 matrix of values. Therefore, each pixel of the image is represented by an ellipsoid and not by a gray level. The segmentation of such an image is not a trivial task, not even for a human. Which ellipsoids should be together in a cluster and which ones do not belong to the first cluster and should form a second cluster? So, instead of trying to answer this question by looking to the tensorial image, the TMG is computed. This step translates the tensorial information into scalars, resulting in a gray-level image (Fig. 2(b)). Finally, all the image analysis, in this example the segmentation (Fig. 2(c)), can be done over an scalar image.

To illustrate the computation of the tensorial morphological gradient of diffusion tensor images, some synthetic tensor fields were created. Real diffusion data was also used. First, results of TMG computation using different tensorial similarity metrics are presented in Section 3.1. Second, distinct structuring elements were tested to compute TMG and the results can be found in Section 3.2. And finally, noise was added to synthetic data. Resulting tensor field and its TMG are shown in Section 3.3 .

3.1 Distinct similarity measures

To run our first experiment, a synthetic diffusion data-set were created. The synthetic diffusion tensor field (Fig. 3(a)) is a 20 X 20 X 20 image where the tensors follow the tangent of the center-line of a torus and share the same eigenvalues. TMG was computed using all similarity measures presented in Section 2.2. Fig. 3(b) and Fig. 3(c) show the TMG computed for the synthetic torus using only two similarity measures: Dot product and Frobenius norm. Both TMG were computed using a 6-connected structuring element (3D).

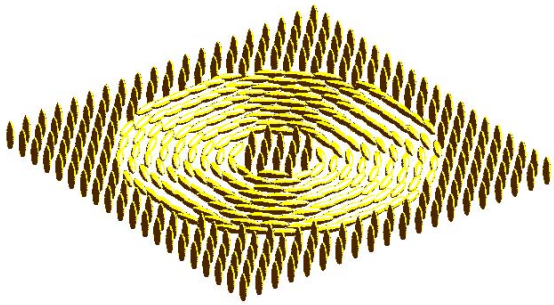

(a) Central slice of synthetic tensor field

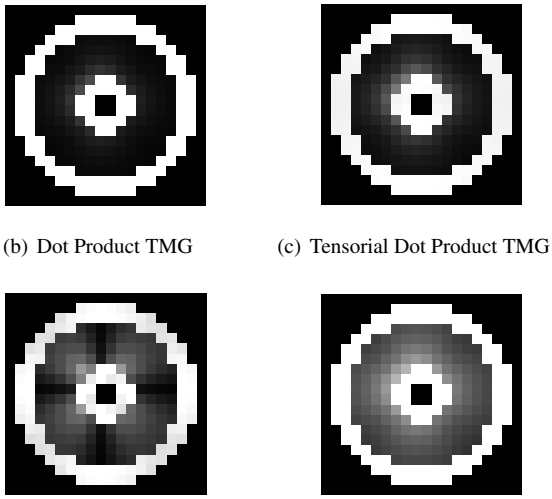

(b) Dot Product TMG (c) Tensorial Dot Product TMG

(d) Frobenius Norm TMG (e) J-divergence TMG

Figure 3. One slice of the a synthetic tensor field (trace and anisotropy constant) and the computed TMGs using four different similarity measures: Dot product, Tensorial dot product, Frobenius norm and J-divergence

Looking at Fig. 3 it is possible to conclude that, for this specific tensor field (torus), all similarity measures tested are adequate to compute the TMG. The dot product (Fig. 3(b)), unappropriate to compute TMG in a tensor field where changes in eigenvalues are more relevant than in eigenvectors, works fine in this example. Since the torus present tensors with constant eigenvalues and the only

[1] Fig.1 partially extracted from [20]

changes are in eigenvectors directions, it is an special circumstance where the TMG using the dot product preserves all necessary information to perform subsequent image processing. Similar behavior is expected from the TMG computed by the tensorial dot product, confirmed by Fig. 3(c).

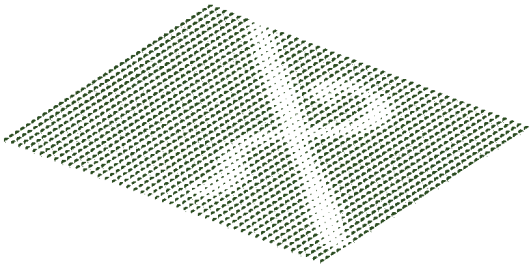

(a) One slice of real DTI (rat spinal cords phantom)

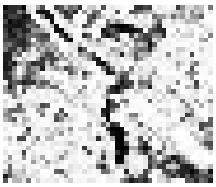

(b) Dot Product TMG

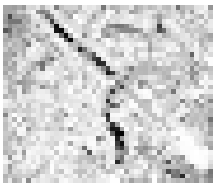

(c) Tensorial Dot Product TMG

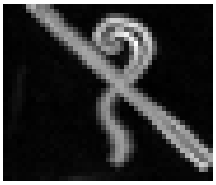

(d) Frobenius Norm TMG

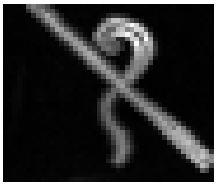

(e) J-divergence TMG

Figure 4. One slice of a real diffusion tensor field (rat spinal cords phantom) and the computed TMGs using four different similarity measures: Dot product, Tensorial dot product, Frobenius norm and J-divergence

Although the Frobenius norm was found as being the most suitable measure to compute the TMG for color images [17], it presents some distortions, as can be seen in Fig. 3(d). The four light gray regions inside the torus derive from the fact that the Frobenius norm is not affine invariant, that is, dissimilarity computed between tensors that are aligned to cartesian axes are different from dissimilarity computed between tensors not aligned to cartesian axes. Conversely, Fig. 3(e) shows that, since the J-divergence is an affine invariant metric, the gray region inside the torus is homogeneously distributed, meaning that the TMG computed presents no distortions due to rotation of the tensors.

Another example of TMG calculation can be found in Fig. 4. Again, the TMG was computed using the same four tensorial similarity measures, but this time the entry was a real diffusion tensor data acquired from a rat spinal cords phantom (Fig. 4(a)) [5]. In this case, computed TMGs using different measures look very distinct. Fig. 4(b) and Fig. 4(c) show that the dot product and the tensorial dot product are not appropriated to compute TMG in a precise manner when dealing with real data, since they take into account only the direction of the principal eigenvector of tensors. Conversely, Fig. 4(d) and Fig. 4(e) confirm that the Frobenius norm and the J-divergence are both more adequate measures to compute the TMG, since they consider the full tensor information. But, unlike previous experiment, it is not clear which measure leads to a better TMG: the Frobenius Norm or the J-divergence. Distortions due to the affine variant characteristic of the Frobenius norm can not be detected. At least, not by a qualitative evaluation of the TMG.

3.2 Distinct structuring elements

All tensorial morphological gradient results presented in previous sections were computed using a 3D 6-connected structuring element. But it is also possible to choose a different neighborhood to compute the tensorial morphological gradient, by changing the structuring element used in the calculation. Any structuring element is admissible, but just a few ones make sense in this application. To illustrate the influence of the structuring element in the TMG computation, three different structuring elements where used: a 4-connected structuring element (2D), a 6-connected structuring element (3D) and a 26-connected structuring element (3D). All TMGs were computed using the Frobenius norm to measure the dissimilarities between tensors.

Fig. 5 depicts the representation of the three structuring elements that were used in this experiment (Fig. 5(a), Fig. 5(c) and Fig. 5(e)). Remember that the gradient is computed for the central voxel, taking into account information contained in the neighborhood defined by the structuring element. Fig. 5(b), Fig. 5(d) and Fig. 5(f) presents the resulting TMGs computed with the different structuring elements, where the influence of the chosen structuring element in the computed gradient can be easily identified. Using the 4-connected structuring element (Fig. 5(a)), the obtained TMG (Fig. 5(b)) takes only into account each slice of data separately, since the structuring element is bidimensional. The result is a thin TMG, good in preserving details of small structures. As the structuring element becomes bigger, or in a higher dimension (Fig. 5(c) and Fig. 5(e)), the borders of the computed tensorial morphological gradient becomes thicker (Fig. 5(d) and Fig. 5(f)). These TMGs are not suitable for detailed structures, but per-

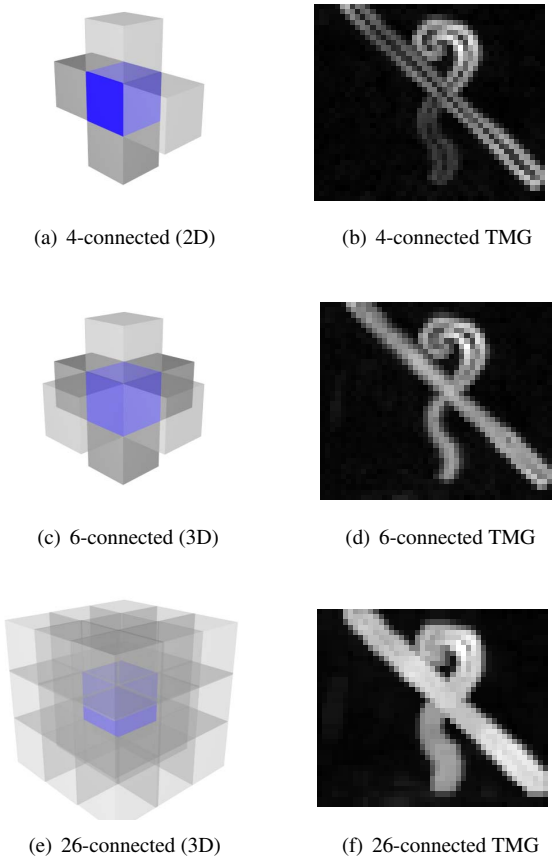

(a) 4-connected (2D) (b) 4-connected TMG (c) 6-connected (3D) (d) 6-connected TMG (e) 26-connected (3D) (f) 26-connected TMG

Figure 5. Different structuring elements and resulting TMGs using each one of the structuring elements

form better if the object to be delineate presents a considerable volume (considerable number of voxels, in comparison to the structuring element) and three-dimensional information is important.

3.3 Noisy data

When dealing with real diffusion tensor images (DTI), noise is one factor that should be take into account. To test the behavior of the TMG in presence of noise, random Gaussian noise was added independently to the three eigenvalues of the synthetic tensor field (torus) in addition to random rotation (in azimuth and elevation) perturbing the three eigenvectors by the same amount to retain orthogonality. This noise addition method adopted here was first reported by Weldeselassie in [20]. In fact, addition of random noise was reported by several DTI segmentation works ([13], [18], [19], [11]), and although the parameters of the noise and the way it is added to tensors vary considerably,

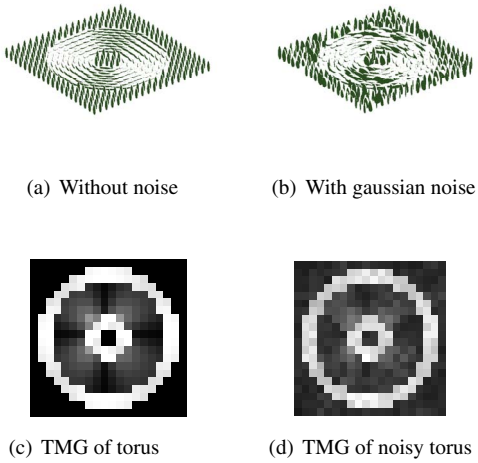

(a) Without noise (b) With gaussian noise (c) TMG of torus (d) TMG of noisy torus

Figure 6. One slice of the torus without and with noise and resulting TMGs

the main idea behind is the same. The purpose is not to simulate real noisy data, but to test the robustness of the segmentation methods in the presence of noise.

Fig. 6(a) and Fig. 6(b) show one slice of the synthetic tensor field without and with noise, respectively. Results of the TMG computed using the Frobenius norm for the synthetic torus without and with noise can be seen in Fig. 6(c) and Fig. 6(d). Despite of the noise added to the tensor field, the obtained TMGs preserved all relevant information, in this case, the borders.

4 Segmentation of diffusion tensor images

Diffusion tensor image segmentation is a challenging task exactly because it has as input a tensorial image and the segmentation method has to decide which information should be considered in segmentation. Furthermore, either existing segmentation methods have to be adapted to deal with tensorial information or completely new segmentation methods have to be developed to accomplish this task. Alternatively, what this work proposes is the computation of a gradient, that transforms the diffusion tensor image into an scalar image, and makes possible the use of any existing method in order to perform the segmentation.

To address the DTI segmentation problem, the IFT-based watershed transform was the method of choice in the field of mathematical morphology. The image foresting transform (IFT) may be seen as a generic approach to project image processing operators, unifying methods such as fuzzy connectedness, watershed transforms, connected operations, distance transforms, and boundary tracking, normally with efficiency gains [9].

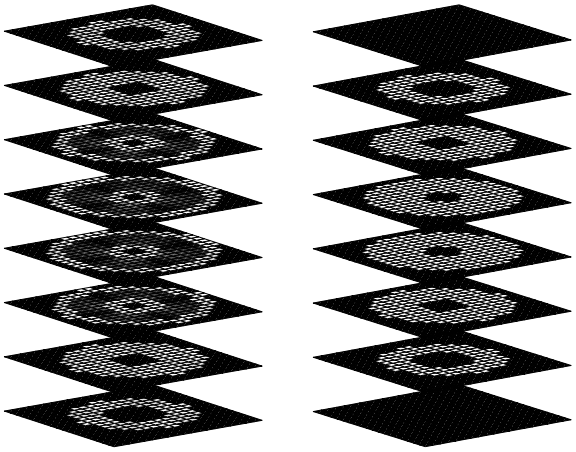

(a) TMG (b) Segmentation result

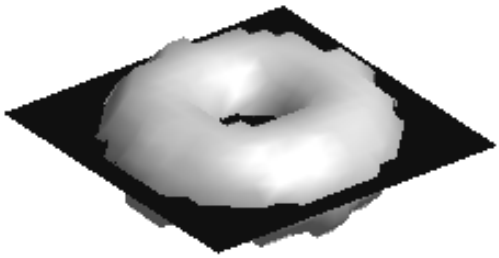

(c) Rendered segmentation result

Figure 7. Computed TMG and watershed segmentation result for a synthetic tensor field (torus) using a 6-neighbor (3D) as the structuring element

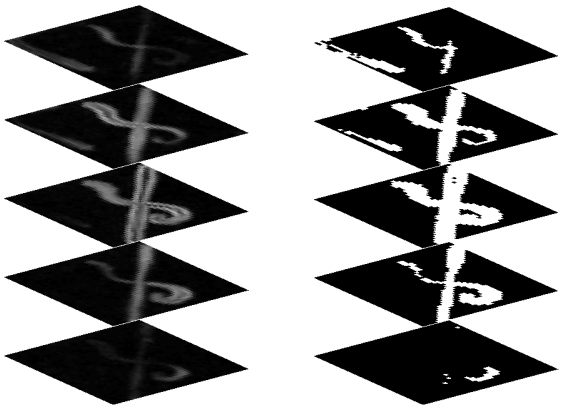

(a) TMG (b) Segmentation result

(c) Rendered segmentation result

Figure 8. Computed TMG and threshold segmentation result for real data (rat spinal cords phantom) using a 6-neighbor (3D) as the structuring elements

In summary, the IFT [10] models the image as a graph, and starting from a given set of seed pixels, uses a given path cost function to partition the image into a minimum-cost path forest. The IFT outputs three parameters for every input pixel, namely: a label corresponding to the closest seed pixel; the predecessor, or parent pixel, in the path; and the cost of that path from the seed up to the pixel. Different IFT-based applications normally use one or a combination of these parameters. In IFT-based watershed transforms [14] the label image represents the influence zones of all the seeds in the optimal image partition.

Fig. 7 illustrates the use of the tensorial morphological gradient and the watershed transform to segment diffusion tensor images. The computed TMG shown in Fig. 7(a) was obtained using a 3D 6-connected structuring element and the Frobenius norm as the tensorial similarity measure. The segmentation was then performed by the watershed transform from markers and its result can be seen in Fig. 7(b). Here the markers used were the regional minima of the TMG. Fig. 7(c) shows the rendered segmentation result.

Although this procedure of computing the TMG of the tensor field and then segmenting it using the watershed transform works well, depending on the data to be segmented, another segmentation method could obtain better results. Fig. 8(a) shows the TMG computed for the real data set already presented in Section 3.1 (Fig. 4(a)). Because the data is composed of thin objects (rat spinal cords), the watershed transform encounters some difficulties, like, for example, finding inner markers. In this case, segmentating by choosing a simple threshold turns out to be more efficient

than using the watershed transform. Fig. 8(b) presents the segmentation result using 40 as the threshold value.

5 Conclusions

This paper proposes the tensorial morphological gradient (TMG) computation of diffusion tensor images, in order to segment them. The TMG processes the tensorial information and transforms it into an scalar image, making possible the use of well known operators from mathematical morphology to segment tensorial images. Experiments were conducted using synthetic and real tensor fields. Distinct similarity functions and structuring elements were tested, and segmentation performed well in all instances.

The strength of the proposed segmentation method is its simplicity and robustness, consequences of the tensorial morphological gradient computation. It enables the use, not only of well known algorithms and tools from the mathematical morphology, but also of any other segmentation method to segment DTI, since the computation of the tensorial morphological gradient transforms tensorial images into scalar ones.

6 Aknowledgments

The authors would like to thank Jennifer Campbell of the McConnell Brain Imaging Centre, Montreal Neurological Institute, McGill University, for the real DTI data sets.

References

[1] D. Alexander, J. Gee, and R. Bajcsy. Similarity measures for matching diffusion tensor images. In *Brit. Mach. Vision Conf.*, 1999.

[2] S. Awate and J. Gee. A fuzzy, nonparametric segmentation framework for dti and mri analysis. In *IPMI*, pages 296–307, 2007.

[3] P. Basser and C. Pierpaoli. Microstructural and physiological features of tissues elucidated by quantitative-diffusion-tensor mri. *J. Magn. Reson.*, 111(3):209–219, June 1996.

[4] R. L. Bishop and S. I. Goldberg. *Tensor Analysis on Manifolds*. Dover, 1980.

[5] J. S. Campbell, K. Siddiqi, V. V. Rymar, A. F. Sadikot, and G. B. Pike. Flow-based fiber tracking with diffusion tensor and q-ball data: validation and comparison to principal diffusion direction techniques. *Neuroimage*, 27(4):725–736, October 2005.

[6] D. A. Danielson. *Vectors and Tensors in Engineering and Physics*. Westview (Perseus), 2003.

[7] A. S. D.K. Jones, M.A. Horsfield. Optimal strategies for measuring diffusion in anisotropic systems by magnetic resonance imaging. *Magn. Reson. Medic.*, 42(3):515–525, 1999.

[8] E. R. Dougherty and R. A. Lotufo. *Hands-on Morphological Image Processing*, volume TT59. SPIE, 2003.

[9] A. Falcão, B. Cunha, and R. Lotufo. Design of connected operators using the image foresting transform. In *Medical Imaging 2001: Image Processing*, volume 4322 of *SPIE Conference*, pages 468–479, July 2001.

[10] A. Falcão, J. Stolfi, and R. Lotufo. The image foresting transform: Theory, algorithms, and applications. *IEEE Trans. Pattern Anal. Mach. Intell.*, 26(1):19–29, Jan. 2004.

[11] R. Z. Freidlin, E. Özarslan, M. E. Komlosh, L.-C. Chang, C. G. Koay, D. K. Jones, and P. J. Basser. Parsimonious model selection for tissue segmentation and classification applications: A study using simulated and experimental dti data. *IEEE Trans. Med. Imag.*, 26(11):1576–1584, 2007.

[12] H. J. A. M. Heijmans. *Morphological Image Operators*. Academic Press, Boston, 1994.

[13] L. Jonasson, P. Hagmann, X. Bresson, R. Meuli, O. Cuisenaire, and J.-P. Thiran. White matter mapping in dt-mri using geometric flows. In *Proc. 9th Intern. Workshop Comput. Aided Syst. Theory*, pages 80–82, Spain, February 2003.

[14] R. Lotufo and A. Falcão. The Ordered Queue and the Optimality of the Watershed Approaches. In *5th International Symposium on Mathematical Morphology*, pages 341–350, Palo Alto (CA), USA, June 2000. Kluwer Academic.

[15] R. Lotufo, A. Falcão, and F. Zampirolli. IFT-watershed from gray-scale marker. In *XV Brazilian Symp. on Computer Graph. and Image Proc.*, pages 146–152, Fortaleza, Brazil, Oct. 2002. IEEE Press.

[16] C. Pierpaoli and P. J. Basser. Toward a quantitative assessment of diffusion anisotropy. *Magn. Reson. Medic.*, 36(6):893–906, 1996.

[17] L. Rittner, F. Flores, and R. Lotufo. New tensorial representation of color images: Tensorial morphological gradient applied to color image segmentation. In *XX Brazilian Symp. on Computer Graph. and Image Proc.*, pages 45–52, Belo Horizonte, Brazil, 2007. IEEE Press.

[18] M. Rousson, C. Lenglet, and R. Deriche. Level set and region based surface propagation for diffusion tensor mri segmentation. In M. Sonka, I. A. Kakadiaris, and J. Kybic, editors, *ECCV Workshops CVAMIA and MMBIA*, volume 3117 of *Lect. Notes Comp. Sci.*, pages 123–134. Springer, 2004.

[19] Z. Wang and B. Vemuri. Dti segmentation using an information theoretic tensor dissimilarity measure. *IEEE Trans. Med. Imag.*, 2005.

[20] Y. Weldeselassie and G. Hamarneh. Dt-mri segmentation using graph cuts. In *Medical Imaging 2007: Image Processing*. SPIE, 2007.

[21] M. Wiegell, D. Tuch, H. Larson, and V. Wedeen. Automatic segmentation of thalamic nuclei from diffusion tensor magnetic resonance imaging. *NeuroImage*, 19:391–402, 2003.

[22] L. Zhukov, K. Museth, D. Breen, R. Whitaker, and A. Barr. Level set modeling and segmentation of dt-mri brain data. *J. Electronic Imaging*, 12:125–133, 2003.

[23] U. Ziyan, D. Tuch, and C. Westin. Segmentation of thalamic nuclei from DTI using spectral clustering. In *MICCAI'06*, Lect. Notes Comp. Sci., pages 807–814, Denmark, 2006.